ADVANCED FUNCTIONAL MATERIALS
www.afm-journal.de

Employing ~100% Excitons in OLEDs by Utilizing a Fluorescent Molecule with Hybridized Local and Charge-Transfer Excited State

Weijun Li, Yuyu Pan, Ran Xiao, Qiming Peng, Shitong Zhang, Dongge Ma, Feng Li, Fangzhong Shen, Yinghui Wang, Bing Yang, and Yuguang Ma**

In principle, the ratio (Φ) of the maximum quantum efficiencies for electroluminescence (EL) to photoluminescence (PL) can be expected to approach unity, if the exciton (bound electron–hole pair) generated from the recombination of injected electrons and holes in OLEDs has a sufficiently weak binding energy. However, seldom are examples of Φ > 25% reported in OLEDs because of the strongly bound excitons for most organic semiconductors in nature. Here, a twisting donor–acceptor triphenylamine-thiadiazol molecule (TPA-NZP) exhibits fluorescent emission through a hybridized local and charge-transfer excited state (HLCT), which is demonstrated from both fluorescent solvatochromic experiment and quantum chemical calculations. The HLCT state possesses two combined and compatible characteristics: a large transition moment from a local excited (LE) state and a weakly bound exciton from a charge transfer (CT) state. The former contributes to a high-efficiency radiation of fluorescence, while the latter is responsible for the generation of a high fraction of singlet excitons. Using TPA-NZP as the light-emitting layer in an OLED, high Φ values of 93% (at low brightness) and 50% (at high brightness) are achieved, reflecting sufficient employment of the excitons in the OLED. Characterization of the EL device shows a saturated deep-red emission with CIE coordinates of (0.67, 0.32), accompanied by a rather excellent performance with a maximum luminance of 4574 cd m^{-2} and a maximum external quantum efficiency (η_{ext}) of ~2.8%. The HLCT state is a new way to realize high-efficiency of EL devices.

1. Introduction

The organic light-emitting diodes (OLEDs) are devices that can convert the injected charges into excitons and then emit photons, which is very promising for the future displays and lighting application.[1–9] A key point is how to achieve a nearly 100% internal quantum efficiency (η_{int}) of electroluminescence (EL) by making full use of both singlet and triplet excitons in OLEDs.[3] It is no longer a novelty in the phosphorescent OLEDs due to the enhanced intersystem crossing (ISC) from spin–orbital interaction in the presence of heavy metal atoms, while only singlet excitons (25% of the total exicitons) contribute to the fluorescent EL according to the spin statistics (singlet/triplet = 1/3).[4] As a consequence, the internal quantum efficiency is limited at 25% in most fluorescent OLEDs, with the triplet excitons (75% of the total excitons) simply wasted as a non-radiative decay to the singlet ground state. To minimize the energy loss from triplet state in fluorescent OLEDs, the final proportion of triplet exciton should be reduced to a minimum. An effective pathway is that, a conversion process from triplet exciton to singlet one is expected to take place.[5] Nowadays, two possible mechanisms have been reported to be capable of this conversion: one is triplet-triplet annihilation (TTA),[6] the other is thermally-activated reverse intersystem crossing (RISC).[7] On the basis of the above two mechanisms, the maximum η_{int} can be raised to 62.5% and 100% respectively in principle. When the thermally-activated RISC happens between the lowest excited state of singlet and triplet, owing to the low ISC rate between triplet and singlet states as well as the long-lifetime nature of the lowest triplet exciton as a result of undergoing a theoretically forbidden process of spin flip, a delayed fluorescence is usually observed, such as thermally-activated delay fluorescence (TADF).[8] Besides, the breakthrough of the 25% limit has also been observed in some π-conjugated polymer systems,[9] due to the delocalized inter-chain charge-transfer (CT) state with a very weak exciton binding energy, but no delay observed in fluorescence. In this contribution, we hope to expand the molecular systems with highly efficient fluorescence and high yield of singlet exciton in OLEDs.

For a pure organic semiconductor, a highly efficient EL requires not only a high fraction of singlet exciton, but also a

Dr. W. J. Li, Dr. Y. Y. Pan, R. Xiao, Dr. Q. M. Peng,
Dr. S. T. Zhang, Prof. F. Li, Dr. F. Z. Shen,
Dr. Y. H. Wang, Prof. B. Yang, Prof. Y. G. Ma
State Key Lab of Supramolecular Structure and Materials
Jilin University
2699 Qianjin Avenue, Changchun, 130012, PR China
E-mail: yangbing@jlu.edu.cn; ygma@jlu.edu.cn
Prof. D. G. Ma
State Key Laboratory of Polymer Physics and Chemistry
Changchun Institute of Applied Chemistry
Chinese Academy of Sciences
Changchun, 130022, PR China

DOI: 10.1002/adfm.201301750

large transition moment or high radiative rate from the emissive state.[3] Intrinsically, the excited state characteristics of the emitter molecules determine their light-emitting properties, e.g. efficiency and energy. CT state is a type of important excited state,[10] in which a couple of coulomb bound hole and electron stay on the donor and acceptor molecules or moieties, corresponding to the inter- or intra-molecular CT, respectively. Generally, CT state shows a very low fluorescent efficiency, due to the characteristic of forbidden electronic transition arising from the full spatial separation of orbitals.[11] On the other hand, the spatially separated electron and hole give rise to a weak binding energy of the CT exciton.[11–13] The binding energy of CT exciton is supposed to be something in between Wannier exciton (radius of ~100 Å, or called free electron and hole) with binding energy of ~10 meV and Frenkel exciton (radius of ~10 Å, or call local excited exciton) with binding energy of ~1.0 eV.[12]] For CT state, the weak binding energy surely induces a larger formation cross section of singlet than triplet, as a result of the small enough singlet-triplet energetic splitting (quasidegenerate singlet and triplet CT excitons).[13,14] Once using a CT-state material as emitter in OLED, a breakthrough in the radiative exciton ratio may be achieved to be larger than 25% of spin statistics. However, the low radiative rate is a key challenge for the CT state to be applied in OLEDs.

In comparison, locally excited-state (LE) is a more efficient radiation state than CT state, arising from its larger transition moment with a larger orbital overlap. It should be an ideal case if we could combine both LE and CT states into a special one, which may possess two combined and compatible characteristics: large transition moment from LE state and weakly bound exciton from CT state. The former contributes to a high-efficiency fluorescence radiative decay, while the latter guarantees the generation of a high fraction of singlet exciton. Using this combined state as an emissive state, the ratio of the maximum quantum efficiencies for electroluminescence (EL) to photoluminescence (PL) can be expected to approach unity, because the full use of both singlet and triplet excitons becomes possible in OLEDs. The twisting donor-acceptor molecule may be an ideal carrier to realize this strategy. An appropriate twisting angle can control the orbital mixing and the interactive LE and CT configuration between donor and acceptor, and thus may produce a special state with the intercrossed LE and CT character,[15] resulting in a full use of both singlet and triplet excitons. Naphtho-[2,3-c][1,2,5]thiadiazole is a strong acceptor moiety, and the linking to triphenylamine at its 4th position can afford a large twisting angle due to the repulsion between neighboring hydrogen atoms, indicating it is a promising constitutional unit for designing a twisting donor-acceptor molecule.

Herein we introduce a deep-red largely twisting D-A molecule *N,N*-diphenyl-4-(9-phenylnaphtho-[2,3-c][1,2,5]thiadiazol-4-yl)aniline (TPA-NZP) with intercrossed LE and CT character, demonstrated by the solvatochromic experiment and density functional theory (DFT) calculation. Further lifetime measurement showed that the intercrossed LE and CT state possessed one lifetime, not two (one for LE, the other one for CT), which indicated that it should be a hybridized local and charge-transfer (HLCT) state. This state may possess both the large dipole of CT state and the large orbital overlap of LE state, or to put it another way, HLCT may be an ideal high-efficiency emissive state. OLED based on it exhibited a highly efficient deep-red EL with a maximum external quantum efficiency η_{ext} of ~2.8%, corresponding to a η_{int}~ 14%.[3,15,16] The high ratio of η_{int}/η_{pl} (93%) in our EL device implies that singlet bound states are formed with higher probability than triplets. As follows, the detailed experimental evidence and theoretical-calculation analysis are present.

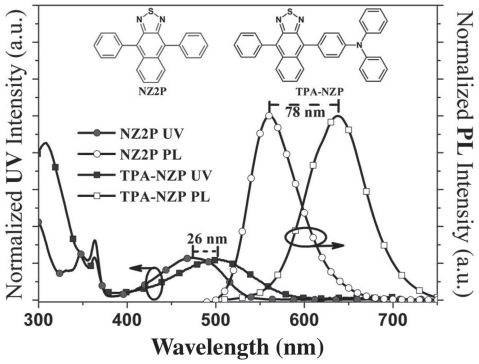

Figure 1. Normalized UV and PL spectra of TPA-NZP in THF (tetrahydrofuran) solution at the concentration of 10^{-5} mol L^{-1} with NZ2P as reference (inset are the molecular structure of TPA-NZP and NZ2P)

2. Results and Discussion

2.1. Excited State Properties

TPA-NZP, as shown in **Figure 1**, is composed of naphtho[2,3-c][1,2,5]thiadiazole (NZ) as the acceptor and TPA as the donor, and obtained as a pure product through a Suzuki coupling reaction (see supporting information). PL measurement showed that TPA-NZP gave a deep-red emission with λ_{max} at 639 nm in the THF solution. Compared to NZ2P (4,9-diphenylnaphtho[2,3-c][1,2,5]thiadiazole), TPA-NZP exhibited obviously large redshifts in UV (26 nm) and PL (78 nm), which may be ascribed to the CT state formation between TPA and NZ moieties. When in different solvents from low-polarity hexane to high-polarity acetone, the fluorescence of TPA-NZP showed an obvious solvatochromic effect with a large redshift of 54 nm, as shown in Figure S1, accompanied by a shift of 13 nm in the UV as well. These shifts, which are commonly consistent with the large dipole moment of a CT state, further indicate that the low-lying excited state, S_1, of the TPA-NZP possesses a certain CT state character.[10]

The dipole moment of the S_1 state can be estimated from the slope of a plot of the Stokes shift (ν_a–ν_f) versus the solvent polarity function *f*, according to the Lippert–Mataga equation.[10] Obviously, the fitted result reflects a non-linear relationship between Stokes shift and solvent polarity, as shown in **Figure 2**. Two independent slopes of the fitted line suggests the existence of two different excited-states, whose dipole moments μ_e, are calculated to be 12.6 D in high-polarity solvents and 6.0 D in low-polarity solvents, respectively, according to the Lippert–Mataga equation (see Supporting Information). The small μ_e of 6.0 D can be attributed to the usual excited-state, which is a

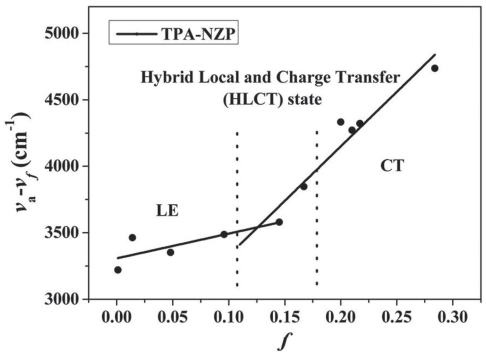

Figure 2. Linear correlation of orientation polarization (f) of solvent media with the Stokes shift (ν_a–ν_f) for TPA-NZP. (See Table S1 for data; the lines in the high- and low-polarity regions were fitted to the points with $f \geq 0.15$ and $f \leq 0.15$, respectively.)

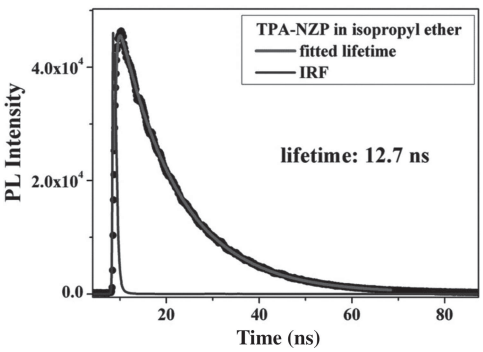

Figure 4. Lifetime measurement of TPA-NZP in moderately polar isopropyl ether solvent by using time-correlated single photon counting method under the excitation of a laser (471.0 nm) with 96.8 ps pulse width.

LE-like state, while the large μ_e of 12.6 D should be treated as a CT-like state.[10] The fluorescent solvatochromic experiments and non-linear relationship of the Stokes shift with solvent polarity indicate that our molecule, TPA-NZP, possesses an intercrossed excited state of LE and CT: a bigger contribution from the CT state in high-polarity solvents ($f \geq 0.2$), whereas a bigger contribution from the LE state in low-polarity solvents ($f \leq 0.1$), and a totally intercrossed excited state of the LE and CT in moderately polar environments between butyl ether and ethyl acetate, or at the polarity level near isopropyl ether. In this case, the hybridized local and charge-transfer (HLCT) state may form due to the intercrossing and coupling between LE and CT states, as shown in **Figure 3**. As the solvent polarity increases, the CT energy level starts to decrease, due to the strong interaction of the solvent field with the CT excited state (large dipole moment), while LE remains nearly unchanged. In low-polarity solvents, the LE dominates the luminescence of HLCT state. With increased solvent polarity, CT part in HLCT state with gradually decreased energy begins to influence the decay transition of HLCT state, resulting in an intercrossed character of LE and CT states. In solvents with very high polarity, the CT may dominate the lowest excited state of HLCT, acting as largely red-shifted CT emissions.

Further lifetime measurement indicated that this intercrossed excited state in the moderately polar solvents should be a hybridized local and charge-transfer (HLCT) state. As shown in **Figure 4**, in the moderately polar isopropyl ether solution, the fitted line of TPA-NZP delay curve gave a single-exponential lifetime of 12.7 ns, determined by the time-correlated single photon counting method under the excitation of a laser (471.0 nm) with a 96.8 ps pulse width. The one lifetime indicated that the intercrossed LE and CT in the moderately polar solvent formed as one hybridized state, not two separated state, as called a hybridized local and charge-transfer state, as shown in Figure 3. This state may possess both the large dipole of CT state and the large orbital overlap of LE state, thus HLCT may be an ideal highly efficient emissive state.

The large twist angle between TPA and NZ moieties is also responsible for the formation of HLCT state. Density functional theory (DFT) calculation reveals that the twist angles are 53.7° and 38.7° for the ground-state and excited-state geometries respectively, by the method of B3LYP/6-31G (d, p). In order to examine the nature of the electronic transitions, natural transition orbitals (NTOs) for the $S_0 \rightarrow S_1$ and $S_0 \rightarrow S_2$ excitations were evaluated at the level of TD-ωB97X/6-31G (d, p) using the geometry of S_0 state, as shown in **Figure 5**. For $S_0 \rightarrow S_1$ excitation, the hole is mainly located on the NZ moiety with a small fraction on TPA moiety, while the particle is obviously localized on the NZ moiety. Thus it contains both a major part of LE transition of NZ and a minor part of CT transition from TPA to NZ unit, corresponding to the HLCT. $S_0 \rightarrow S_2$ transition is also a HLCT property with the major CT composition and the minor LE. The dipole moments of S_1 and S_2 states are estimated to be 6.6 D and 15.7 D respectively, which is in good agreement with those evaluated from the Lippert–Mataga equation. From a potential surface scan in Figure S2, the accessible angular range of twist angles is 40–75° at room temperature (k_BT) in the ground state of TPA-NZP. With a decreasing twist angle, the orbital coupling and mixing are enhanced between donor and acceptor units (Figure S3 and Table S2), which contributes to the change of HLCT (S_1 and S_2 states) property through the mixing ratio between LE and CT compositions. Importantly, S_1 state shows much larger oscillator strength than S_2 state as a result of the major LE character, which is necessary for high efficiency fluorescence (Table S2). Solvent effect was taken into account using the PCM (polarizable continuum model) method, the

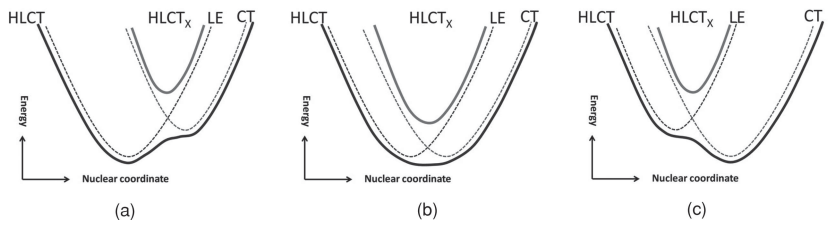

Figure 3. Scheme of LE and CT states intercross to form a hybridized local and charge-transfer state (HLCT) in a) low polarity, b) medium polarity, c) high polarity of solvents.

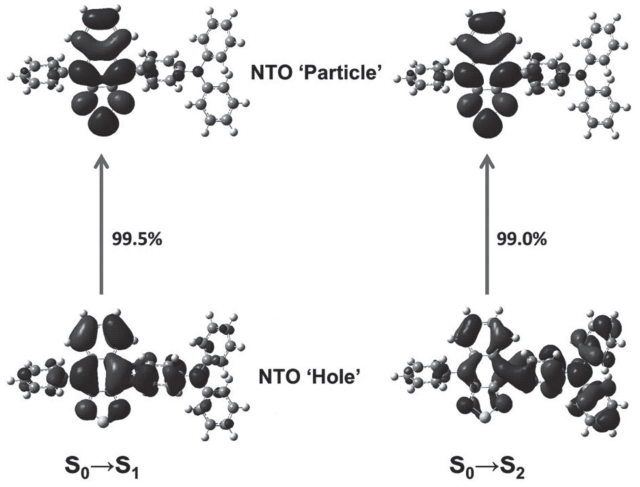

Figure 5. Natural transition orbitals (isovalue surface 0.02 a.u.) for $S_0 \rightarrow S_1$ and $S_0 \rightarrow S_2$ excitation from tuned TD-ωB97X ($\omega = 0.15$ bohr^{-1}) for the TPA-NZP at the S_0 state geometry. The weight of the hole-particle contribution to the excitation also included.

calculated absorption and emission were consistent with those in the experiment (Table S3). In addition, we also calculated the singlet-triplet energy splitting (ΔE_{ST}) for TPA-NZP at the S_1 state geometry (Table S4). Obviously, S_2 state with dominant CT character give rises to the smaller ΔE_{ST} than that of S_1 state. Combined with high fluorescent emission and small singlet-triplet energy splitting (ΔE_{ST}), HLCT is a promising solution for material design of the new-generation OLEDs.

The film state emission of TPA-NZP shows a similar character (λ_{max} at 632 nm) to those in moderately polar solvents, as shown in Figure S4, thus a HLCT state may be formed in TPA-NZP film as well. By an integrating-sphere photometer, the photoluminescent efficiency of TPA-NZP film was estimated to be ~ 15% (±3%) on average.

2.2. Electroluminescence Properties

To investigate the EL properties, we constructed a device with a frequently used multilayered structure: indium tin oxide (ITO)/ MoO_3 (10 nm)/*N,N*′-di-1-naphthyl-*N,N*′-diphenylbenzidine (NPB) (80 nm)/4,4′,4″-tri(*N*-carbazolyl)-triphenylamine (TCTA) (5 nm)/TPA-NZP (20 nm)/1,3,5-tri(phenyl-2-benzimidazolyl)-benzene (TPBi) (40 nm)/LiF (1 nm)/Al (100 nm), in which MoO_3 was utilized as a hole-injecting layer, NPB and TCTA as hole-transporting and buffer layers, and TPBi as an electron-transporting and hole-blocking layer. As shown in **Figure 6**a, the EL spectra showed a saturated deep-red emission with a CIE coordinate of (0.67, 0.32), which is stable in the whole drive voltage range from 5V to 10V. This device exhibited an excellent performance with a maximum luminance of 4574 cd m^{-2}, maximum current efficiency of ~1.3 cd A^{-1}, maximum power efficiency of ~1.1 lm W^{-1}, and maximum external quantum efficiency (η_{ext}) of ~2.8%, which were among the best results reported[17] currently, as shown in Figure S5. Through calculation from the relationship $\eta_{ext} = \eta_{int} \cdot \eta_{ph}$, assuming a light

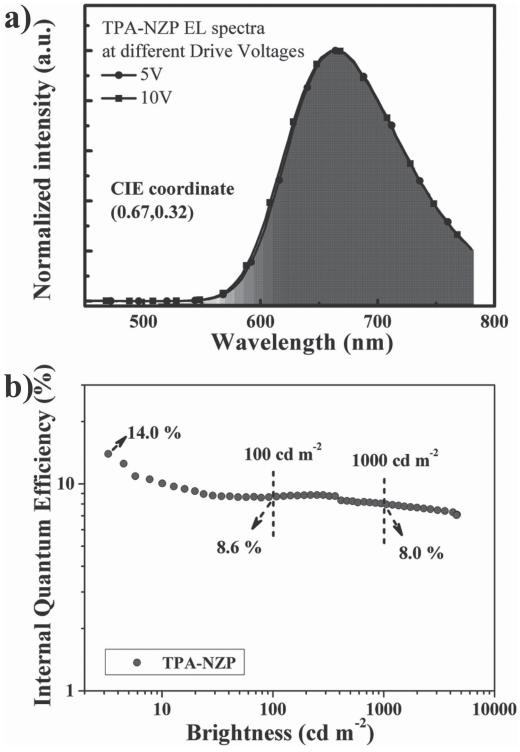

Figure 6. a) The EL spectra at different drive voltages and b) the internal quantum efficiency–luminance curves of non-doped EL device with TPA-NZP as the emitter.

out-coupling efficiency of $\eta_{ph} \approx 1/(2\ n^2) \approx 20\%$ for a glass substrate with an index of refraction $n = 1.5$, we tuned the η_{ext} to the corresponding maximum internal quantum efficiency η_{int} of ~14%.[3] Considering the TPA-NZP fluorescent quantum efficiency of 15%, this meant that nearly 93% excitons (obtained from 14%/15%) of electron-hole recombination were employed in TPA-NZP device, largely breaking through the limit of 25% of spin statistics (singlet/triplet ratio ~ 1/3). Even at the brightness of 100 or 1000 cd m^{-2}, the η_{ext} still kept among the best results of non-doped deep-red OLEDs at 1.7% or 1.6%,[17] which corresponded to a η_{int} of 8.5% or 8.0%, respectively, as shown in Figure 6b. It indicated that the radiative exciton ratio still kept above 50% under the high luminance, which is twice of the limit of 25%. This breakthrough of radiative exciton ratio could be ascribed to the TPA-NZP emitter with a HLCT state character.

The EL delay in TPA-NZP non-doped device was measured under a transient electric voltage with a pulse width of 10 μs, with $Ir(PPQ)_2acac$ doped one as reference, in the same device structure of ITO/NPB(40 nm)/TPA-NZP (30 nm) or $Ir(PPQ)_2acac$:MCP (3%, 30 nm) /TPBi (50 nm)/LiF (1 nm)/Al (100 nm), as shown in **Figure 7**. When electric voltage was off (at ~10 μs), in the short-time range (10 μs & time & 10.5 μs), the EL delay was determined mainly by the radiative decay of excitons formed before voltage off. In this range, TPA-NZP based device exhibited a sharp decay curve compared to $Ir(PPQ)_2acac$, which was consistent with their respective radiative curve of excitons under photo excitation. In the

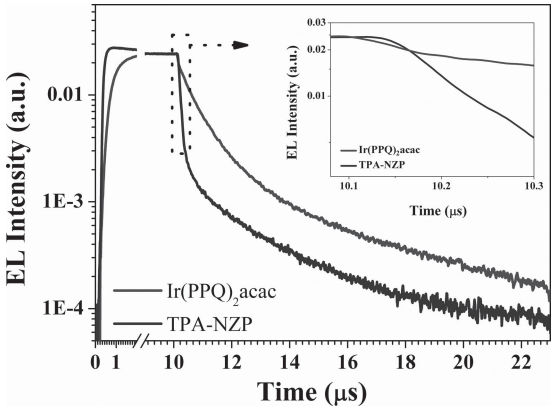

Figure 7. EL delay of TPA-NZP nondoped and $Ir(PPQ)_2acac$ doped OLED under the transient electric voltage (repetition: 1 kHz; width: 10 μs).

long-delay time range of > 12 μs, the EL delay could be attributed to the collision recombination[18] of previously injected hole and electrons which stayed in the emitter layer after voltage off, and here TPA-NZP and $Ir(PPQ)_2acac$ displayed the similar delay curve. The long-time delayed decays up to microsecond scale from the exciton transition of triplet to singlet as a TADF or triplet–triplet annihilation (TTA) process were not observed in the TPA-NZP device.[5,6,8] Thus the probable reason for the high singlet exciton ratio in our device could be attributed to the RISC process through the high-lying CT_X state[5] in the TPA-NZP emitter, as shown in **Figure 8**a.

When the injected holes and electrons recombine in the TPA-NZP light-emitting layer, they initially form singlet (^1CT_x) and triplet (^3CT_x) states with a ratio of 1/3, including both intermolecular and intramolecular CT_X states. Due to a near-zero or even inverse singlet-triplet energy splitting (ΔE_{ST}), the possible RISC or spin mixing[13,19] may happen between ^1CT_x and ^3CT_x in the high-lying CT_X states, provided that k_{ISC} is faster than k_{3CT}, as well as k_{1CT} is larger than k_{3CT}.[20] Thus S_1 exciton may be finally obtained with a higher probability than T_1, resulting in the radiative exciton ratio to break through the limit of 25% in TPA-NZP device. Through TDDFT calculation, an extraordinarily large energy gap (1.8 eV from ωB97X and 1.27 eV from B3LYP with the similar energy landscape) was estimated between T_2 and T_1 states in TPA-NZP, as shown in Figure 8b. This large energy gap may significantly decrease the internal conversion rate from T_2 to T_1, which may lead to comparable rates between k_{3CT} from T_2 to T_1 and k_{ISC} from T_2 to S_2 (the enhanced ISC rate from the small singlet-triplet energy splitting ΔE_{ST}, as a result of HLCT with the dominant CT character in both T_2 and S_2 states). Meanwhile, the large energy barrier between T_1 and S_1 prevents the RISC from long-lifetime T_1 to S_1, due to HLCT with the dominant LE character in both T_1 and S_1 states. Thus in TPA-NZP case, a RISC process may be possible through the higher intermolecular CT_x state or intramolecular T_2 to S_2 state, and induces the terminal singlet exciton ratio to exceed 25% of spin statistic in OLEDs. Actually, through applying an external magnetic field on OLEDs, negative magnetic field effects (MELs) were obtained, giving an experimental evidence for the RISC effect.[21] Therefore, in our TPA-NZP based EL device, the reason for the high singlet exciton ratio could be attributed to the RISC process in the high-lying CT_X state.

3. Conclusion

Photophysical and DFT analysis demonstrated that a deep-red twisting D–A molecule TPA-NZP showed a hybrid local and charge-transfer state character with an obvious CT feature in the excited state, which provided a weak binding energy and resulted in a larger singlet/triplet ratio than 1/3 of spin statistic. By using TPA-NZP as an emitter in a non-doped multilayered EL device, a high radiative exciton proportion of >50% was obtained in the nearly whole range of brightness (≤ 1000 cd m^{-2}), which largely exceeded the limit of 25% of spin statistic (singlet/triplet: ~ 1/3). Our results showed a promising method by using HLCT state to construct the highly efficient OLEDs, which may catch up with the current phosphorescent one in the near future.

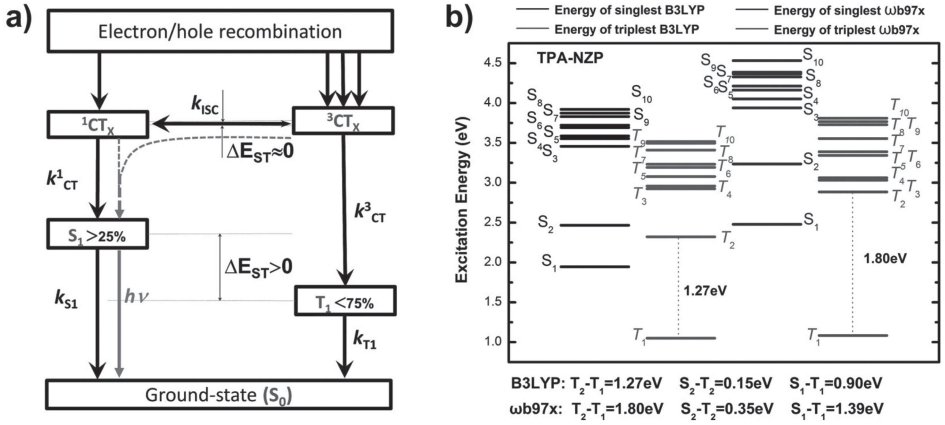

Figure 8. a) The illustration of exciton forming process of emitter from hole and electron recombination in electric excitation condition of OLEDs. b) The energy landscape of singlet and triplet excited states from TD calculation using B3LYP and ωB97X functional, respectively.

Supporting Information

Supporting Information is available from the Wiley Online Library or from the author.

Acknowledgements

We are grateful for support from the National Science Foundation of China (51073069, 51273078), the Ministry of Science and Technology of China (2009CB623605, 2013CB834801), and PCSIRT (20921003).

Received: May 22, 2013
Revised: August 11, 2013
Published online: October 29, 2013

[1] C. W. Tang, S. A. VanSlyke, *Appl. Phys. Lett.* **1987**, *51*, 93.
[2] Y. G. Ma, H. Zhang, J. C. Shen, C. Che, *Synth. Met.* **1998**, *94*, 245.
[3] C. Adachi, M. A. Baldo, S. R. Forrest, M. E. Thompson, *J. Appl. Phys.* **1999**, *11*, 285.
[4] a) S. J. Su, E. Gonmori, H. Sarabe, J. Kido, *Adv. Mater.* **2008**, *20*, 4189; b) F. M. Hsu, C. H. Chien, C. F. Shu, C. H. Lai, C. C. Hsieh, K. W. Wang, P. T. Chou, *Adv. Funct. Mater.* **2009**, *19*, 2834; c) Y. Tao, Q. Wang, C. L. Yang, C. Zhong, K. Zhang, J. G. Qin, D. G. Ma, *Adv. Funct. Mater.* **2010**, *20*, 304; d) S. O. Jeon, S. E. Jang, H. S. Son, J. Y. Lee, *Adv. Mater.* **2011**, *23*, 1436.
[5] a) S. Reineke, M. A. Baldo, *Phys. Status. Solidi A* **2012**, *12*, 2341; b) A. P. Monkman, *ISRN Materials Science* **2013**, DOI: 10.1155/2013/670130.
[6] Y. C. Luo, H. Aziz, *Adv. Funct. Mater.* **2010**, *20*, 1285.
[7] K. Goushi, K. Yoshida, K. Sato, C. Adachi, *Nat. Photonics* **2012**, *6*, 253.
[8] a) A. Endo, K. Sato, K. Yoshimura, T. Kai, A. Kawada, H. Miyazaki, C. Adachi, *Appl. Phys. Lett.* **2011**, *98*, 083302; b) H. Uoyama, K. Goushi, K. Shizu, H. Nomura, C. Adachi, *Nature* **2012**, *492*, 234.
[9] a) Y. Cao, I. D. Parker, G. Yu, C. Zhang, A. J. Heeger, *Nature* **1998**, *397*, 414; b) M. Wohlgenannt, K. Tandon, S. Mazumdar, S. Ramasesha, Z. V. Vardeny, *Nature* **2001**, *25*, 494; c) Z. Shuai, D. Beljonne, R. J. Silbey, J. L. Brédas, *Phys. Rev. Lett.* **2000**, *84*, 131.
[10] Z. R. Grabowski, K. Rotkiewicz, W. Rettig, *Chem. Rev.* **2003**, *103*, 3899.
[11] A. D. Gorse, M. Pesquer, *J. Phys. Chem.* **1995**, *99*, 4039.
[12] M. Pope, C. E. Swenberg, *Electronic Processes in Organic Crystals and Polymers*, Oxford University Press, Oxford **1999**.
[13] a) M. Segal, M. Singh, K. Rivoire, S. Difley, T. V. Voorhis, M. A. Baldo, *Nat. Mater.* **2007**, *6*, 374; b) S. Difley, D. Beljonne, T. V. Voorhis, *J. Am. Chem. Soc.* **2008**, *130*, 3420.
[14] A. Kadashchuk, A. Vakhnin, I. Blonski, D. Beljonne, Z. Shuai, J. L. Brédas, V. I. Arkhipov, P. Heremans, E. V. Emelianova, H. Bässler, *Phys. Rev. Lett.* **2004**, *93*, 066803.
[15] W. J. Li, D. D. Liu, F. Z. Shen, D. G. Ma, Z. M. Wang, T. Feng, Y. X. Xu, B. Yang, Y. G. Ma, *Adv. Funct. Mater.* **2012**, *22*, 2797.
[16] N. C. Greenham, R. H. Friend, D. D. C. Bradley, *Adv. Mater.* **1994**, *6*, 491.
[17] a) Y. S. Yao, J. Xiao, X. S. Wang, Z. B. Deng, B. W. Zhang, *Adv. Funct. Mater.* **2006**, *16*, 709; b) L. Chen, B. H. Zhang, Y. X. Cheng, Z. Y. Xie, L. X. Wang, X. B. Jing, F. S. Wang, *Adv. Funct. Mater.* **2010**, *20*, 3143.
[18] a) D. J. Pinner, R. H. Friend, N. Tessler, *Appl. Phys. Lett.* **2000**, *76*, 1137; b) K. O. Cheon, J. Shinar, *Phys. Rev. B* **2004**, *69*, 201306.
[19] W. Barford, R. J. Bursill, D. V. Marhov, *Phys. Rev. B* **2010**, *81*, 035206.
[20] W. Barford, *Phys.Rev. B* **2004**, *70*, 205204.
[21] Q. M. Peng, W. J. Li, S. T. Zhang, P. Chen, F. Li, Y. G. Ma, *Adv. Optical Mater.* **2013**, DOI: 10.1002/adom.201300028.